Finding a Curve of Space by its Cyclographic Image

Tatyana Myasoedova [1], Konstantin Panchuk [1] and Evgeniy Lyubchinov [1]

[1] *Omsk State Technical University, Mira, h. 11, Omsk, 644050, Russia*

Abstract

The present paper explores the questions of development and practical application of the constructive method of geometric modeling. In particular, the paper justifies possibility of solution to the inverse problem of cyclographic mapping of a curve of space R^3, i.e. reconstruction of a spatial curve given its cyclographic projection. It is proven that knowing either orthogonal and one of the two branches of the cyclographic projection of a curve of space R^3 in plane $z = 0$, or both of its branches, is sufficient to determine a curve of space. The spatial curve, its orthogonal and cyclographic projections have common parameterization, which allows one to establish point-to-point bijection between these three elements and perform solutions of the direct and the inverse problems of cyclographic modeling of a spatial curve. The paper formulates and establishes theses justifying the possibility of analytic solution of practical tasks of cyclographic modeling, for example, cutting tool trajectory calculation for high-precision pocket machining of machine-building products on NC units. The algorithm for solution to the inverse problem is demonstrated on examples.

Keywords

Cyclographic mapping, medial axis, medial transformation axis, inverse task, α-shell, vertex points of the curve.

1. Introduction

Cyclographic modeling of geometric objects is based on bijection that is established, in its simplest form, between a multitude of points R^3 and a multitude of cycles in plane z = 0 [1,2]. Presently, due to the high technology level of computer graphics and CAD, the cyclographic method, while complex and approximate in manual constructive realization, is more and more successful at finding application in theoretic geometric studies [1,2] as well as in practical solutions to the problems of geometric optics [1,3,4], road surface form design [2,3], surface processing in mechanical engineering [3,5], etc.

The theory of cyclographic modeling of a spatial curve studies the direct and the inverse problems of modeling. The direct problem consists in construction of cyclographic projection of a given spatial curve [1,2,3], while the inverse problem constitutes spatial reconstruction of a curve given its cyclographic projection [2,4]. Combined, a curve of space R^3, its orthogonal and cyclographic projections in plane z = 0 form a triad of geometric elements, where knowing any two elements out of three is necessary and sufficient to define the unknown third element [4]. Elements of the triad have common parameterization, which allows one to establish point bijection between the elements and solve both direct and inverse problems.

The inverse problem is often applied in formation of equidistant curves used as cutting tool trajectories in pocket surface machining on NC units [3,5,6]. Its existing solutions are performed directly in plane z = 0 through methods based on approximate calculus [7,8,9,10].

2. Inverse problem of cyclographic modeling of a spatial curve

In order to fully understand the inverse problem of cyclographic modeling of a spatial curve, let us consider geometric scheme of construction of its cyclographic projection (Figure 1). A spatial curve

GraphiCon 2022: 32nd International Conference on Computer Graphics and Vision, September 19-22, 2022, Ryazan State Radio Engineering University named after V.F. Utkin, Ryazan, Russia
EMAIL: mtm44mtm44@mail.ru (T. Myasoedova); panchuk_kl@mail.ru (K. Panchuk); Lubchinov.E.V@yandex.ru (E. Lyubchinov)
ORCID: 0000-0002-9641-9417 (T. Myasoedova); 0000-0001-9302-8560 (K. Panchuk); 0000-0003-2499-4866 (E. Lyubchinov)

$\overline{p}(t) = (x(t), y(t))$ with parameter t is correspondent to a triad of lines on plane z = 0: an orthogonal projection $\overline{p}_1(t)$, a cyclographic projection $\overline{p}_{C1}(t)$ and $\overline{p}_{C2}(t)$. Here $\overline{p}(t)$ is the prototype, while the pair of elements of the triad $\overline{p}_{C1}(t)$ and $\overline{p}_{C2}(t)$ constitute the image of the curve $\overline{p}(t)$ in cyclographic representation. The direct problem of modeling, i.e. $\overline{p}(t) \to (\overline{p}_{C1}(t), \overline{p}_{C2}(t))$, is considerably more thoroughly studied in scientific publications than the inverse problem $(\overline{p}_{C1}(t), \overline{p}_{C2}(t)) \to \overline{p}(t)$. In particular, if $(\overline{p}_{C1}(t) \cup \overline{p}_{C2}(t)) = \overline{p}_C(t)$ is a closed curve, which is the case in the relevant problem of cutting tool trajectory calculation in pocket machining, the urgent question is whether it is at all possible to calculate the geometric object fundamental for such calculation – the line $\overline{p}(t)$. Justification of this possibility consists in selecting an appropriate method of division of the closed contour $\overline{p}_C(t)$ into segments $\overline{p}_{C1}(t)$ and $\overline{p}_{C2}(t)$. Obviously, such division must engage the vertex points of the contour $\overline{p}_C(t)$ affecting its geometry.

The objective of this study consists in development of new algorithms of inverse task solution based on cyclographic mapping of a spatial curve, simpler and more computationally available compared to the algorithms currently known.

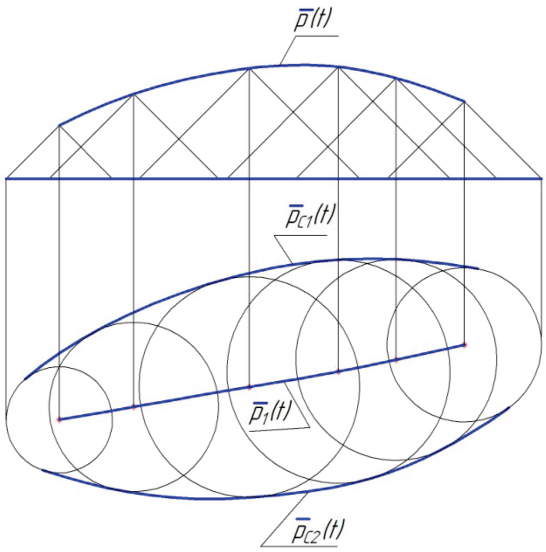

Figure 1: Cyclographic projection of curve $\overline{p}(t)$ generation scheme

2.1. Theory

Let us consider the theoretical aspects of solution of the inverse problem of cyclographic modeling of a spatial curve. The theory is based on the following statements.

***Statement* 1**. For any simple closed plane curve there is a unique spatial curve to which the first curve serves as a cyclographic projection.

Let us verify this statement. A simple closed plane curve $\overline{p}_c(t) = (x_c(t), y_c(t))$, $T_0 \le t \le T$ in plane $z = 0$ is given. Let us divide this curve into two segments: $\overline{p}_{c_1}(t_1) = (x_{c_1}(t_1), y_{c_1}(t_1))$, $T_{01} \le t_1 \le T_1$ and $\overline{p}_{c_2}(t_2) = (x_{c_2}(t_2), y_{c_2}(t_2))$, $T_{02} \le t_2 \le T_2$. Obviously, there is more than one method of such division; the guidelines to optimal division will be considered later. For each of the curve segments let us construct evolutes $\overline{p}_{e_1}(t_1) = (x_{e_1}(t_1), y_{e_1}(t_1))$ and $\overline{p}_{e_2}(t_2) = (x_{e_2}(t_2), y_{e_2}(t_2))$ through the equations known in differential geometry

$$\overline{p}_{e_1}(t_1) = \overline{p}_{c_1}(t_1) + \frac{1}{k_{c_1}(t_1)}\overline{n}_{c_1}(t_1),\ \overline{p}_{e_2}(t_2) = \overline{p}_{c_2}(t_2) + \frac{1}{k_{c_2}(t_2)}\overline{n}_{c_2}(t_2),$$

where k_{c_i} represents curvature, $\overline{n}_{c_i}$ represents normal, i = 1,2.

For each of the evolutes let us construct a spatial image:

$$\begin{aligned}\overline{p}_{E_1}(t_1) &= \left(x_{e_1}(t_1), y_{e_1}(t_1), z_{e_1}(t_1) = \pm\sqrt{(x_{c_1}(t_1)-x_{e_1}(t_1)^2+(y_{c_1}(t_1)-y_{e_1}(t_1)^2)}\right),\\ \overline{p}_{E_2}(t_2) &= \left(x_{e_2}(t_2), y_{e_2}(t_2), z_{e_2}(t_2) = \pm\sqrt{(x_{c_2}(t_2)-x_{e_2}(t_2)^2+(y_{c_2}(t_2)-y_{e_2}(t_2)^2)}\right).\end{aligned} \quad (1)$$

Then let us construct the respective α-surfaces [1]:

$$\begin{aligned}\overline{P}_{\alpha_1}(t_1,l_1) &= \overline{p}_{E_1}(t_1)+l_1(\overline{p}_{c_1}(t_1)-\overline{p}_{E_1}(t_1)),\\ \overline{P}_{\alpha_2}(t_2,l_2) &= \overline{p}_{E_2}(t_2)+l_2(\overline{p}_{c_2}(t_2)-\overline{p}_{E_2}(t_2))\end{aligned}, \quad (2)$$

The equations for α-surfaces $\overline{P}_{\alpha_1}$ and $\overline{P}_{\alpha_2}$ in combination define the curve of intersection $\overline{P}_{\alpha_1} \cap \overline{P}_{\alpha_2}$ that constitutes the *MAT* curve. Indeed, we can see that the cyclographic projections of the curve of intersection $\overline{P}_{\alpha_1} \cap \overline{P}_{\alpha_2}$ belonging to the surfaces $\overline{P}_{\alpha_1}$ and $\overline{P}_{\alpha_2}$ are the respective curves $\overline{p}_{c_1}$ and $\overline{p}_{c_2}$ in plane z = 0. The orthogonal projection of the curve of intersection $\overline{P}_{\alpha_1} \cap \overline{P}_{\alpha_2}$ is the curve $\overline{p}_1$. In the geometric scheme of cyclographic surface formation the curve $\overline{p}_1$ is a multitude of centres of all possible cycles tangent to the curves $\overline{p}_{c_1}$ and $\overline{p}_{c_2}$ simultaneously. Therefore the multitude of cycles inscribed into a domain of plane z = 0 bounded by curves $\overline{p}_{c_1}$ and $\overline{p}_{c_2}$ constitutes a cyclographic image of a multitude of points of curve of intersection $\overline{P}_{\alpha_1} \cap \overline{P}_{\alpha_2}$ in plane z = 0. Since every α-surface is unique, as follows from the geometric scheme of cyclographic mapping $\overline{p}_{c_1} \to \overline{P}_{\alpha_1}$, $\overline{p}_{c_2} \to \overline{P}_{\alpha_2}$, there can be only one pair of surfaces $\overline{P}_{\alpha_1}$ and $\overline{P}_{\alpha_2}$, and only one curve of intersection $\overline{P}_{\alpha_1} \cap \overline{P}_{\alpha_2}$.

Therefore the curve $\overline{P}_{\alpha_1} \cap \overline{P}_{\alpha_2}$ is a line of space R^3 to which the given curve $\overline{p}_c(t)$ serves as a cyclographic projection.

It is worth noting that in the general case the solution of the system of equations for the curves of intersection of α-surfaces $\overline{P}_{\alpha_1}(t_1,l_1)$ and $\overline{P}_{\alpha_2}(t_2,l_2)$ is not analytic unlike the solution to the problem of punctual construction of the curve of intersection $\overline{P}_{\alpha_1} \cap \overline{P}_{\alpha_2}$ defined as a discrete multitude of points of intersection of straight generatrices of one of the α-surfaces with the other [2].

It is preferable to perform division of the curve $\overline{p}_c(t)$, that constitutes a simple closed convex contour $\partial(\Omega)$ of a domain of plane z = 0, using the vertex points of the curve $\overline{p}_c(t)$. The division of the closed contour is based on the theorem of four vertices of a simple plane curve [11], i.e. any smooth simple closed curve in Cartesian plane has at least four vertices. This theorem is true for both convex and non-convex closed contours. The vertices of a smooth plane curve are the extremum points of its curvature. In the general case, when the curvature function has no degenerated points of curvature, i.e. the points where the second derivative is equal to zero, the closed curve has an even number of vertices with alternating maximum and minimum curvature values.

***Statement* 2**. For an open-ended simple plane curve there exists a multitude of spatial curves for which the first curve serves as a cyclographic projection.

Let $\overline{p}_c(t)$ be an open-ended simple curve in plane z = 0 as shown on Figure 2, left. Let us construct its evolute $\overline{p}_e(t)$ and its spatial image $\overline{p}_E(t)$ defined by parametric equations (1). Let us now construct an α-surface defined by parametric equations, e.g. (2), see figure 2, right. Obviously, the cyclographic image in plane z = 0 of any possible curve belonging to the α-surface is one and the same line $\overline{p}_c(t)$.

Conclusions:

1. Introduction of a functional dependence $l = f(t)$, where $f(t)$ is the function of homeomorphic mapping $I \leftrightarrow L$, where $I:[T_0 \le t \le T]$, $L:[l_0 \le l \le l_n]$, into the equation (2) singles out a curve of the α-surface (2) for which the given curve $\overline{p}_c(t)$ serves as a cyclographic projection. Obviously, the function *f(t)* is not unique.

2. Introduction of an additional simple open-ended curve $\overline{p}_1(\omega)$ of plane $z = 0$ as an orthogonal projection of a certain curve on the α-surface (2) lets us define a single curve of space for which $\overline{p}_c(t)$ serves as a cyclographic projection. This follows from the mentioned properties of a triad of curves $\overline{p}_1(t)$, $\overline{p}_{c_1}$, and $\overline{p}_{c_2}$.

Consequently, under these conditions the inverse problem of cyclographic mapping for the case of open-ended curve can be formulated as follows: it is required to construct a curve given its open-ended (incomplete) cyclographic and orthogonal projections in plane $z = 0$. In this task the spatial curve fulfills the role of an image, while the pair of curves in plane $z = 0$ serve as the prototypes of reverse cyclographic mapping.

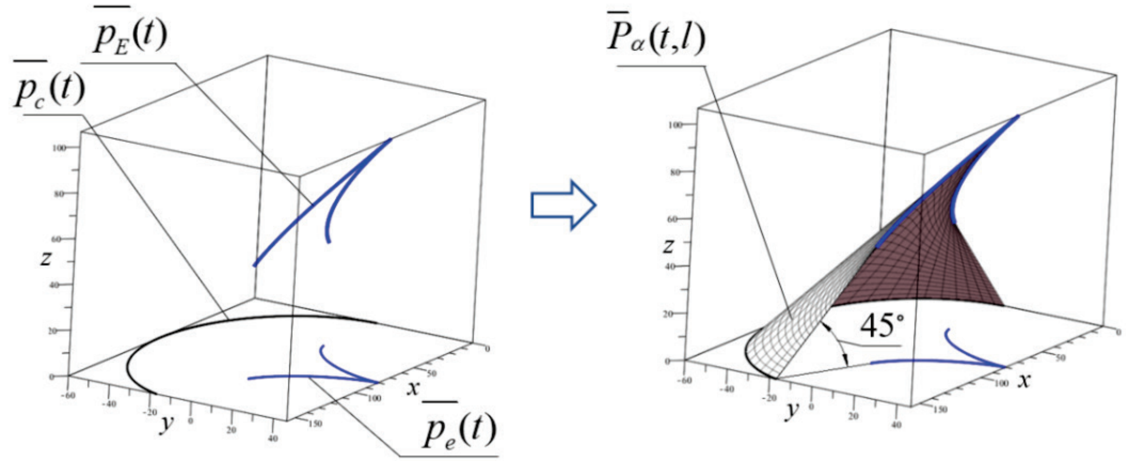

Figure 2: α-surface formation

Let us consider the parametric equations $x_c = x_c(t)$, $y_c = y_c(t)$ for cyclographic mapping [2, 7] of a spatial curve $\overline{p}(t) = (x(t), y(t), z(t))$, $T_0 \le t \le T$. It can be noted that at $D > 0$, where $D = (x'(t))^2 + (y'(t))^2 - (z'(t))^2$, the cyclographic image $\overline{p}_c(t) = (x_c(t), y_c(t))$ includes two real components $\overline{p}_{c_1}(t)$ and $\overline{p}_{c_2}(t)$ that can either connect generating a closed curve in plane $z = 0$, or not connect and remain mutually dependent with respect to parameter *t*. It is irrelevant here that the orthogonal projection $\overline{p}_1(t) = (x(t), y(t))$ of the curve $\overline{p}(t)$ is a single-parameter multitude of centres of cycles with envelope $\overline{p}_c(t)$. The curves $\overline{p}_1(t)$, $\overline{p}_{c_1}(t)$, $\overline{p}_{c_2}(t)$ in plane $z = 0$ form a triad where, as pointed out above, any curve is unambiguously determined by the other two [4]. The particularities of geometric construction of form generation of the curve $\overline{p}_c(t)$ and the mutual parametric dependence of the specified curves of the triad need to be considered in solution of both direct $\overline{p}(t) \to \overline{p}_c(t)$ and inverse $\overline{p}_c(t) \to \overline{p}(t)$ problems of cyclographic modelling. Reasoning from the above general particularities and properties of geometric construction of cyclographic modelling of a spatial curve, let us consider the possibility of solution to the inverse problem given $\overline{p}_c(t)$ in the form of a simple closed convex curve. In the theory of the inverse problem $\overline{p}_c(t) \to \overline{p}(t)$, it is conventional to name the curve $\overline{p}(t)$ '*MAT*' (*Medial Axis Transformation*), and its orthogonal projection $\overline{p}_1(t)$ '*MA*' (*Medial Axis)* [6,7,8]. In the modern studies the solution of the direct and the inverse problems is performed in plane $z = 0$ with application of various apparatus and technologies of geometric and mathematical modelling [5, 7, 8, 9, 10]. The existing solutions are generally performed with scheme $\overline{p}_c(t) \to MA \to MAT$ and based on approximate calculations.

In the present paper a different approach to solving the considered inverse task is proposed. This approach is based on the most simple computations for the problem and application of the space R^3. Let us consider the examples.

2.2. Results of experiments

Example 1. A given boundary contour of a domain $\partial(\Omega)$ is given in the form of an ellipse, see Figure 3. It is required to determine the *MAT* curve.

Let us divide the contour ellipse into two segments $\overline{p}_1(t_{p_1})$ and $\overline{p}_2(t_{p_2})$, and express their parametric equations $\overline{p}_1(x_{p_1}(t_{p_1}), y_{p_1}(t_{p_1}))$ and $\overline{p}_2(x_{p_2}(t_{p_2}), y_{p_2}(t_{p_2}))$. They are of the following form:

$$x_{p_1} = a_1\frac{2t_{p_1}}{1+t_{p_1}^2}, y_{p_1} = b_1\frac{1-t_{p_1}^2}{1+t_{p_1}^2}, -1 \le t_{p_1} \le 1, a_1 = 4, b_1 = 2;$$

$$x_{p_2} = a_2\frac{2t_{p_2}}{1+t_{p_2}^2}, y_{p_2} = -b_2\frac{1-t_{p_2}^2}{1+t_{p_2}^2}, -1 \le t_{p_2} \le 1, a_2 = 4, b_2 = 2.$$

Since an ellipse has four vertices, let us further divide each of the segments $\overline{p_1}(t_{p_1})$ and $\overline{p_2}(t_{p_2})$ into two elementary segments with respect to parameters t_{p_1} and t_{p_2}, as shown on figure 3:

$$\overline{p_1}(t_{p_1}) = \overline{p_{c_1}}(t_1) \cup \overline{p_{c_2}}(t_2), \ -1 \le t_1 \le 0, \ 0 \le t_2 \le -1 \ ,$$

$$\overline{p_2}(t_{p_2}) = \overline{p_{c_3}}(t_3) \cup \overline{p_{c_4}}(t_4), \ -1 \le t_3 \le 0, \ 0 \le t_4 \le -1 \, .$$

Let us then determine the equations for elementary segments $\overline{p_{c_i}}(t_i)$ between points T_i and T_{i+1}, where T_i is the vertex of the curve serving as the initial point of an elementary segment of the ellipse, T_{i+1} is the next vertex of the curve serving as the final point of an elementary segment of the ellipse. The elementary segments are formed as follows: $\overline{p_{c_1}}(t_{p_1}), -1 \le t_{p_1} \le 0$ and $\overline{p_{c_2}}(t_{p_1}), 0 \le t_{p_1} \le 1$; $\overline{p_{c_3}}(t_{p_2}), -1 \le t_{p_2} \le 0$ and $\overline{p_{c_4}}(t_{p_2}), 0 \le t_{p_2} \le 1$, where $t_{Ti} \le t_{p_i} \le t_{Ti+1}$; t_i is the current parameter of the segment T_iT_{i+1}; $t_i = (1-\lambda)\cdot t_{Ti} + \lambda\, t_{Ti+1}$; $0 \le \lambda \le 1$. The equations for the four elementary segments of an ellipse are of the following form:

$$\overline{p}_{c_1}(t_1): \quad x_{c_1} = \frac{8t_1}{1+t_1^2}, y_{c_1} = \frac{1-t_1^2}{1+t_1^2}, 0 \le t_1 \le 1;$$

$$\overline{p}_{c_2}(t_2): \quad x_{c_2} = \frac{8(1-t_2)}{(1-t_2)^2+1}, y_{c_2} = \frac{2((1-t_2)^2+1)}{(1-t_2)^2+1}, 0 \le t_2 \le 1;$$

$$\overline{p}_{c_3}(t_3): \quad x_{c_3} = \frac{8(1-t_3)}{(1-t_3)^2+1}, y_{c_3} = -\frac{2(1-(1-t_3)^2)}{(1-t_3)^2+1}, 0 \le t_3 \le 1;$$

$$\overline{p}_{c_4}(t_4): \quad x_{c_4} = \frac{8t}{1+t_4^2}, y_{c_2} = -\frac{2(1-t_4^2)^2}{1-t_4^2}, 0 \le t_4 \le 1.$$

Let us now express the parametric equations for spatial images of evolutes $\overline{p}_{E_1}(t_1)$, $\overline{p}_{E_2}(t_2)$, $\overline{p}_{E_3}(t_3)$, and $\overline{p}_{E_4}(t_4)$ of the elementary segments $\overline{p_{c_i}}(t_i), i = 1,2,3,4$ (see Figure 4) based on the equations $x_E = x_e$, $y_E = y_e$, $z_E = \sqrt{(x_c - x_E)^2 + (y_c - y_E)^2}$, where $x_e(t), y_e(t)$ are the parametric equations for an elementary segment evolute. Let us proceed with formation of *α*-surfaces $\overline{P}_{\alpha_1}(t_1,l_1)$, $\overline{P}_{\alpha_2}(t_2,l_2)$, $\overline{P}_{\alpha_3}(t_3,l_3)$, and $\overline{P}_{\alpha_4}(t_4,l_4)$ on the basis of the general *α*-surface equation $\overline{P}_{\alpha_1}(l,t) = \overline{p_c}(t) + l(\overline{p_E}(t) - \overline{p_c}(t))$ with certain parametric expressions for coordinates for each of the *α*-surfaces.

Technically, the line of intersection of two parametrically defined *α*-surfaces is acquired by solution of a system of three equations in four unknown. In the considered case the intersecting *α*-surfaces are $\overline{P}_{\alpha_1} = (x_{\alpha_1}(t_1,l_1), y_{\alpha_1}(t_1,l_1), z_{\alpha_1}(t_1,l_1))$ and $\overline{P}_{\alpha_4} = (x_{\alpha_4}(t_4,l_4), y_{\alpha_4}(t_4,l_4), z_{\alpha_4}(t_4,l_4))$. In order to acquire the line of their intersection, it is required to express the four unknown parameters t_1, l_1, t_4, and l_4, through one of the two unknown parameters l_1 and l_4:

$$\begin{cases} x_{\alpha_1}(t_1,l_1) = x_{\alpha_4}(t_4,l_4), \\ y_{\alpha_1}(t_1,l_1) = y_{\alpha_4}(t_4,l_4), \\ z_{\alpha_1}(t_1,l_1) = z_{\alpha_4}(t_4,l_4). \end{cases}$$

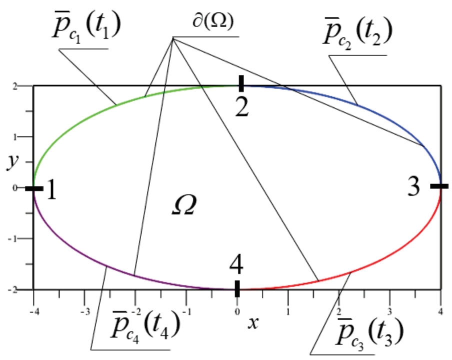

Figure 3: Boundary contour $\partial(\Omega)$ - an ellipse of four elementary segments $\overline{p}_{c_1}(t_1) \cup \overline{p}_{c_2}(t_2) \cup \overline{p}_{c_3}(t_3) \cup \overline{p}_{c_4}(t_4)$

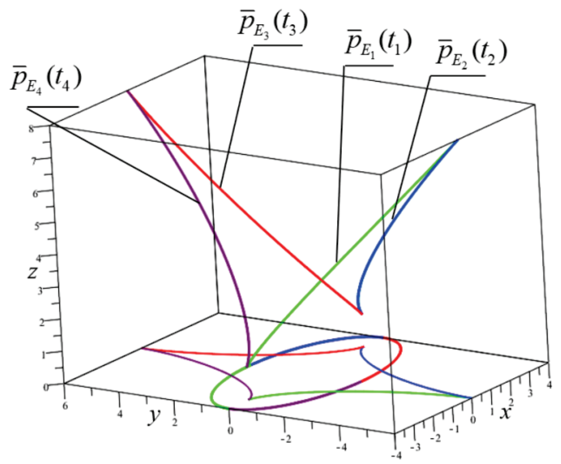

Figure 4: Spatial image of evolute of an ellipse

Since we consider the intersection of two ruled surfaces, the solution of the system of equations can be performed by finding functional dependencies of parameters of the system of equations. For example, let us first find the function of parameter l_1, namely $l_1(t_1,t_4,l_4)$, from the equation $z_1(t_1,l_1) = z_4(t_4,l_4)$ with the aid of symbolic calculus feature of *Maple* software. Then, also through *Maple* software, let us determine the functional dependence of parameter l_4, namely $l_4(t_1,t_4)$, from the equation $y_1(t_1,l_1(t_1,t_4,l_4)) = y_4(t_4,l_4)$. Then we express the function of parameter t_4 by solving a system of equations $x_1(t_1,l_1) = x_4(t_4,l_4)$, where $l_1(t_1,t_4,l_4)$ and $l_4(t_1,t_4)$ are the parameter functions. This is the way we acquire the parameter functions $l_4(t_1,l_1)$, $t_4(t_1,l_1)$, and $l_1(t_1,t_4,l_4)$. By substitution of the parameter function $l_1(t_1,t_4,l_4)$ into the equation for *α*-surface $\overline{P}_{\alpha_1} = (x_{\alpha_1}(t_1,l_1), y_{\alpha_1}(t_1,l_1), z_{\alpha_1}(t_1,l_1))$ we acquire the parametric equations for the curve $\overline{MAT}_1(t_1)$ of intersection of the surfaces $\overline{P}_{\alpha_1}(t_1,l_1)$ and $\overline{P}_{\alpha_4}(t_4,l_4)$, see Figures 5, 6:

$$\overline{MAT}_1 = (x_{MAT_1}(t_1), y_{MAT_1}(t_1), z_{MAT_1}(t_1)) = \overline{P}_{\alpha_1}(t_1,l_1) \cap \overline{P}_{\alpha_4}(t_4,l_4),\ t_1 \in [0,1], t_4 \in [0,1], l_1 \in [0,1], l_4 \in [0,1].$$

Through functional dependence of parameters we can express parameter function $t_1(t_4,l_4)$, and then determine parameter functions $l_1(t_4,l_4)$, $t_4(t_1,l_1)$, and $l_4(t_4,t_1,l_1)$. By substitution of the function $l_4(t_4,t_1,l_1)$ into the equation for *α*-surface $\overline{P}_{\alpha_4} = (x_{\alpha_4}(t_4,l_4), y_{\alpha_4}(t_4,l_4), z_{\alpha_4}(t_4,l_4))$ we acquire the parametric equations for the curve $\overline{MAT}_4(t_4)$ of intersection of surfaces $\overline{P}_{\alpha_1}(t_1,l_1)$ and $\overline{P}_{\alpha_4}(t_4,l_4)$, see Fgures 5, 6:

$$\overline{MAT}_4 = \overline{P}_{\alpha_1}(t_1,l_1) \cap \overline{P}_{\alpha_4}(t_4,l_4), \overline{MAT}_4 = (x_{MAT_4}(t_4), y_{MAT_4}(t_4), z_{MAT_4}(t_4)),\ t_1 \in [0,1], t_4 \in [0,1], l_1 \in [0,1], l_4 \in [0,1].$$

I the same way, solving the system of equations

$$\begin{cases} x_{\alpha_2}(t_2,l_2) = x_{\alpha_3}(t_3,l_3), \\ y_{\alpha_2}(t_2,l_2) = y_{\alpha_3}(t_3,l_3), \\ z_{\alpha_2}(t_2,l_2) = z_{\alpha_3}(t_3,l_3), \end{cases}$$

we find the curves $\overline{MAT}_2(t_2)$ and $\overline{MAT}_3(t_3)$, see Figures 4, 5:

$$\overline{MAT}_2 = \overline{P}_{\alpha_2}(t_2,l_2) \cap \overline{P}_{\alpha_3}(t_3,l_3), \overline{MAT}_2 = (x_{MAT_2}(t_2), y_{MAT_2}(t_2), z_{MAT_2}(t_2)),$$
$$t_2 \in [0,1], t_3 \in [0,1], l_2 \in [0,1], l_3 \in [0,1];$$
$$\overline{MAT}_3 = (\overline{P}_{\alpha_2}(t_2,l_2) \cap \overline{P}_{\alpha_3}(t_3,l_3), \overline{MAT}_3 = (x_{MAT_3}(t_3), y_{MAT_3}(t_3), z_{MAT_3}(t_3)),$$
$$t_2 \in [0,1], t_3 \in [0,1], l_2 \in [0,1], l_3 \in [0,1].$$

The parametric equations for curves $\overline{MAT}_1$, $\overline{MAT}_2$, $\overline{MAT}_3$ and $\overline{MAT}_4$ are acquired through the functional dependence of parameters t_1, l_1, t_4, and l_4. The resultant expressions are too cumbersome to present them in print; one can download these calculations and view them in *Maple* following the link below: https://www.mapleprimes.com/posts/213421-Spline-Curves-Formation-Given-Extreme-Derivatives?sp=213421.

As a result of the calculations, we acquire the *MAT* curve for the contour of a domain bounded by an ellipse. The *MAT* constitutes a composite curve:

$$MAT = \overline{MAT}_1 \cup \overline{MAT}_3 = \overline{MAT}_4 \cup \overline{MAT}_2 = \overline{MAT}_1 \cup \overline{MAT}_2 = \overline{MAT}_4 \cup \overline{MAT}_3 .$$

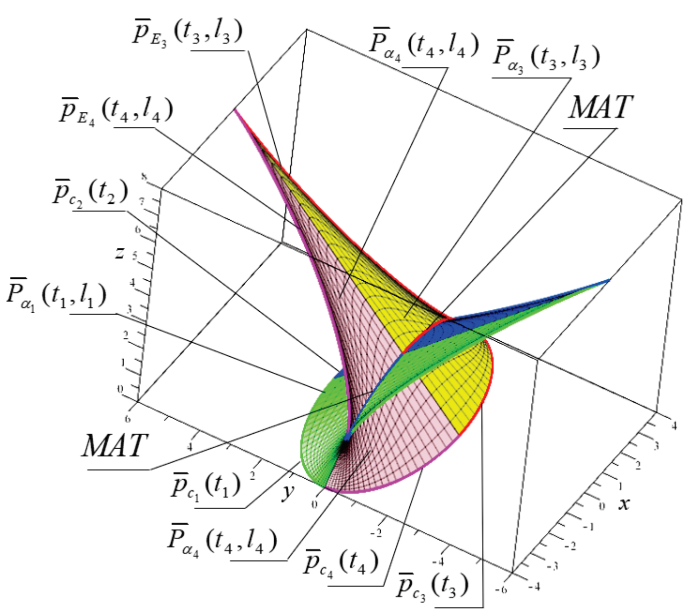

Figure 5: MAT formation visualization

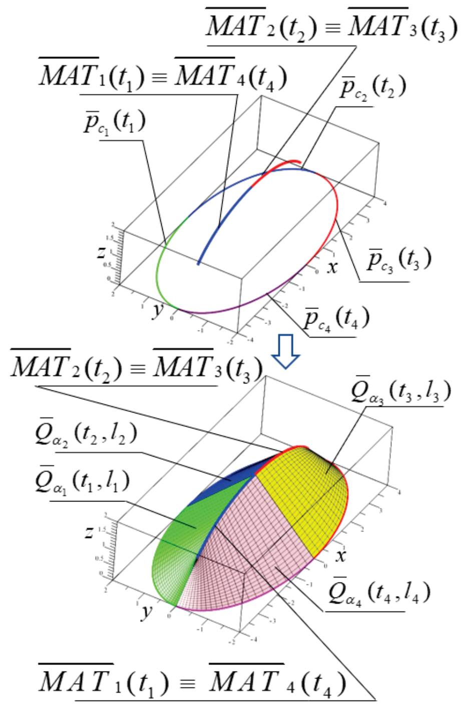

Figure 6: Composite α-shell formation visualization

Example 2. Let us consider construction of a convex boundary contour of a domain $\partial(\Omega)$ based on a cyclic homogenous cubic *B*-spline given knot points (-3, 5); (0, 8); (6, 10); (7, 5); (3, 3); (-3, 5); let us then construct the *MAT* curve for this contour.

It is known that a *B*-spline curve is defined by the following expression [11, 12]:

$$\overline{p}(t) = \sum_{i=0}^{n} \overline{T}_i N_{i,k}(t), \quad \mathrm{u}_{\min} \le t \le u_{\max},$$

where the i^{th} normalized basis function $N_{i,k}(t)$ of order k is defined recursively by the Cox – de Boor formula:

$$N_{i,k}(t) = \frac{(t-u_i)N_{i,k-1}(t)}{u_{i+k-1}-u_i} + \frac{(u_{i+k}-t)N_{i+1,k-1}(t)}{u_{i+k}-u_{i+1}},$$

$$N_{i,k}(t) = \begin{cases} 1 & \text{if } u_i \le t \le u_{i+1} \\ 0 & \text{otherwise,} \end{cases}$$

where $u_i \le u_{i+1}$ represent knot interval borders for parameter t, where the basis function $N_{i,k}(t)$ has non-zero values; k represents basis function degree; $k-1$ is elementary B-spline degree; $n+1$ represents the number of knots; $[u_0, u_1, \ldots, u_{m-1}]$ defines knot vector. The knot vector is the basic object of B-spline curve construction. A total of $m = n + k + 1$ particular knot values of the normalized knot vector are spread on equal distances. In order to construct a cyclic (closed) B-spline curve, it is required to repeat $k-2$ vertices at the initial and the final points of the closed polygon defined by the given knots. In our current example $n = 5$, $k = 4$. In order to construct a closed B-spline curve, let us repeat two knots for further calculations: (-3, 5); (0, 8); (6, 10); (7, 5); (3, 3); (- 3, 5); (0, 8); (6, 10); then $n = 7$, $m = 7 + 4 + 1 = 12$. Therefore the following is true for each knot vector:

$$[1 \quad 2 \quad 3 \quad 4 \quad 5 \quad 6 \quad 7 \quad 8 \quad 9 \quad 10 \quad 11 \quad 12]$$

$$[u_0 \quad u_1 \quad u_2 \quad u_3 \quad u_4 \quad u_5 \quad u_6 \quad u_7 \quad u_8 \quad u_9 \quad u_{10} \quad u_{11}]$$

The number of elementary B-splines taking part in B-spline curve construction does not match the number of knot vector intervals. The curve is evaluated within effective intervals only. Auxiliary knots do not affect the resultant approximating curve, but rather allow us to construct and apply a complete set of elementary B-splines in B-spline curve calculation. The following condition is true for the effective intervals of the uniform knot vector with zero-based indices and integer incrementation: $k-1 \le t \le n+1$ [11]. In this example the indexing is one-based, therefore the effective intervals are defined by the interval $k-1+1 \le t \le n+1+1$, hence $4 \le t \le 9$. The parametric equations for segments $\overline{p_i} = (x_{p_i}(t), y_{p_i}(t))$ of the boundary contour $\partial(\Omega)$ filling the effective intervals ($4 \le t \le 5$, $5 \le t \le 6$, $\ldots, 8 \le t \le 9$) are of the following form:

$$\overline{p_5} \qquad x_{p_5} = -\frac{35}{2} + \frac{9}{2}t + \frac{3}{2}(t-4)^2 - \frac{4}{3}(t-4)^3,$$

$$y_{p_5} = -\frac{13}{6} + \frac{5}{2}t - \frac{1}{2}(t-4)^2 - (t-4)^3,\ 4 \le t \le 5;$$

$$\overline{p_6} \qquad x_{p_6} = -\frac{37}{3} - \frac{5}{2}(t-5)^2 + \frac{7}{2}t,$$

$$y_{p_6} = \frac{49}{3} - \frac{3}{2}t - \frac{7}{2}(t-5)^2 + \frac{5}{3}(t-5)^3,\ 5 \le t \le 6;$$

$$\overline{p_7} \qquad x_{p_7} = \frac{91}{6} - \frac{3}{2}t - \frac{5}{2}(t-6)^2 + \frac{1}{2}(t-6)^3,$$

$$y_{p_7} = \frac{53}{2} - \frac{7}{2}t + \frac{1}{6}(t-6)^3 + \frac{3}{2}(t-6)^2,\ 6 \le t \le 7;$$

$$\overline{p_8} \qquad x_{p_8} = \frac{113}{3} - 5t - (t-7)^2 + \frac{11}{6}(t-7)^3,$$

$$y_{p_8} = \frac{11}{3} + 2(t-7)^2 - \frac{1}{2}(t-7)^3,\ 7 \le t \le 8;$$

$$\overline{p_9} \qquad x_{p_9} = \frac{21}{2} - \frac{3}{2}t + \frac{9}{2}(t-8)^2 - (t-8)^3,$$

$$y_{p_9} = -\frac{89}{6} + \frac{5}{2}t + \frac{1}{2}(t-8)^2 - \frac{1}{3}(t-8)^3,\ 8 \le t \le 9.$$

The evaluated closed convex B-spline curve is presented on Figure 7; it has six vertices with alternating maximum and minimum curvature values as shown on Figure 8.

The calculated vertex points of curve $\partial(\Omega)$ allow us to divide it into three segments 6- 1- 2, 2- 3- 4, 4- 5- 6. The borders of these segments are the three vertex points 2, 4, 6 of maximum curvature. These segments are accepted as the first directrices of the three α-surfaces (by the number of pairs of vertices 6-2, 2-4, 4-6 of maximal curvature). The second directrices of these α-surfaces are spatial images of respective evolutes. Further division of the acquired *B*-spline curve into segments this time limited only by vertex points requires reparametrization of the curve. It is worth noting that this division does not affect the resultant *MAT* geometry.

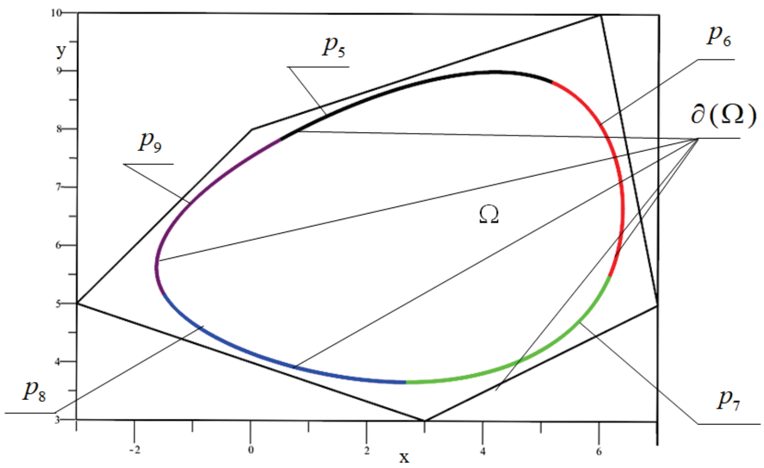

Figure 7: Boundary contour $\partial(\Omega)$ in the shape of a B-spline curve

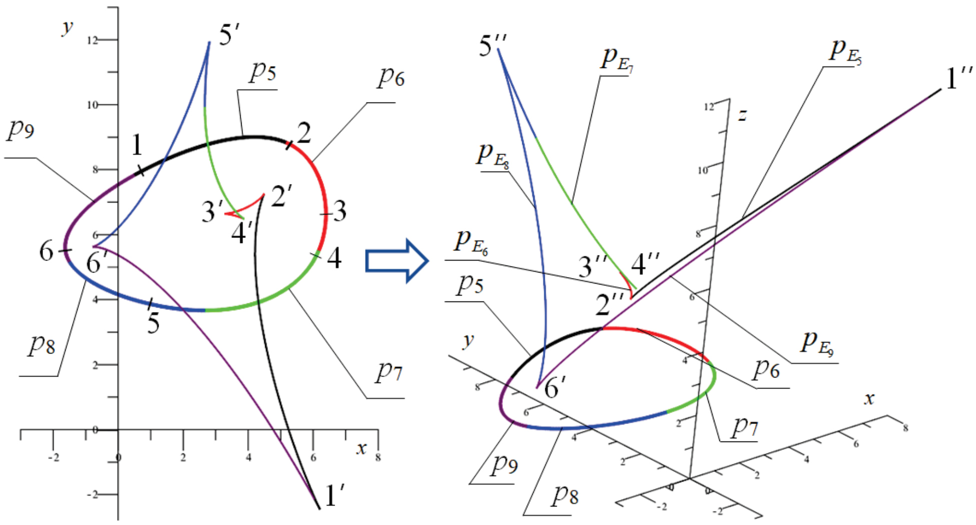

Figure 8: Boundary contour $\partial(\Omega)$ in the shape of a B-spline curve

Consideration of pairs of second directrices of the three constructed *α*-surfaces 6''-1''-2'', 2''-3''-4'', 4''-5''-6'' allows us to determine their common points 2'', 4'', 6''. These points correspond to the maximum curvature points of *B*-spline curve $\partial(\Omega)$ and therefore can belong to the sought *MAT* curve. At the same time, orthogonal projections of peak points 1'', 3'', 5'' (points of z_{max}) of each of these directrices constitute in plane $z = 0$ vertex points of minimal curvature.

Of the three points 2'', 4'', 6'' two points 2'' and 6'' correspond to the vertex points 2 and 6 of the contour $\partial(\Omega)$ with higher curvature than the point 4. Besides, points 2'' and 6'' are, as follows from the evolute 1'-2'-3'-4'-5'-6', boundary points of the sought *MAX* curve for the given contour $\partial(\Omega)$. Point 4'' does not belong to the *MAT* curve as follows from the calculation results and Fgure 9. The results of the conducted calculations are visualized on Figure 10.

This example confirms existence of a *MAT* curve of a convex contour $\partial(\Omega)$ in the form of a *B*-spline curve, due to the existence of points 2' and 6' belonging to this curve. The *MAT* curve is acquired as a multitude of points of intersection of straight lines of the *α*-surfaces. In order to do that, through the general equation $\overline{P}_{\alpha_i}(t,l_i)=\overline{p_i}(t)+l_i(\overline{p_{E_i}}(t)-\overline{p_i}(t))$ we perform preliminary analytic formation of α-surfaces $\overline{P}_{\alpha_5}(t,l_5)$, $\overline{P}_{\alpha_6}(t,l_6)$, $\overline{P}_{\alpha_7}(t,l_7)$, $\overline{P}_{\alpha_8}(t,l_8)$, and $\overline{P}_{\alpha_9}(t,l_9)$, where $\overline{p_i}(t)$ and $\overline{p_{E_i}}(t)$ are parametric equations for segments and spatial images of the evolutes of these segments defined by formulas $x_{Ei}=x_{e_i}(t)$, $y_{E_i}=y_{e_i}(t)$, $z_{E_i}(t)=\sqrt{(x_{p_i}-x_{E_i})^2+(y_{p_i}-y_{E_i})^2}$.

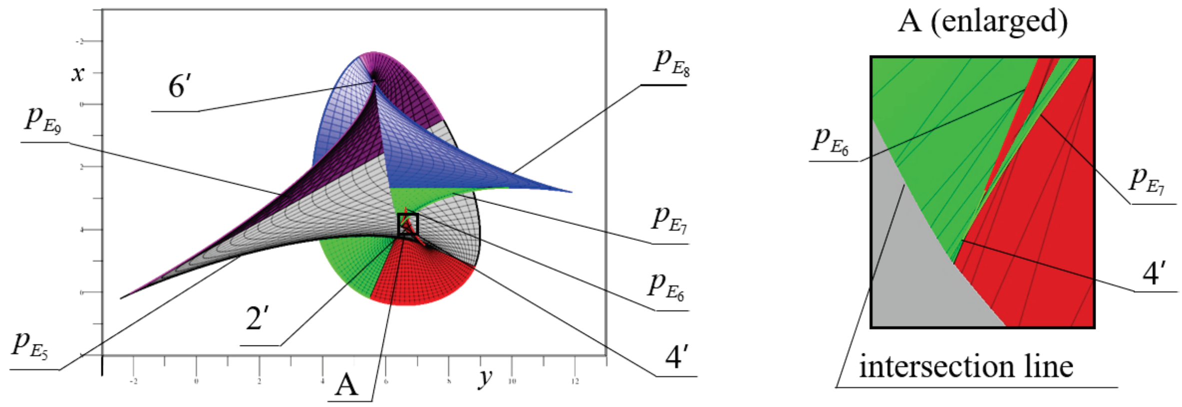

Figure 9: Visualization of intersection of the α-surfaces

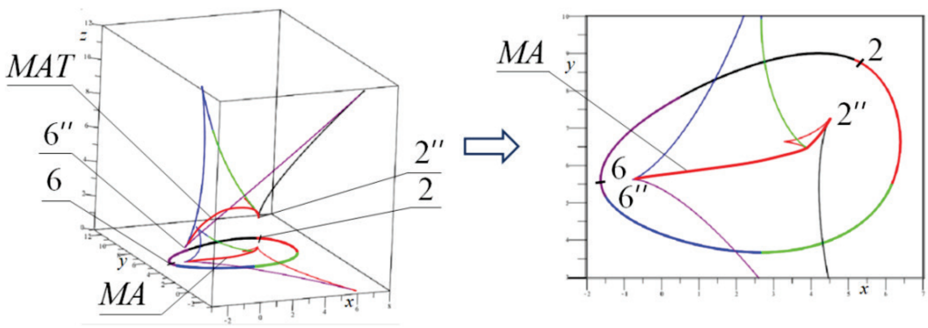

Figure 10: Visualization of the calculated *MAT* curve

The analysis of the calculations presented in examples 1 and 2 allows us to come to the following conclusions:

1. Given a boundary contour $\partial(\Omega)$ in the form of separate second-degree curves or outlines of their segments, it is possible to produce an analytical solution to the inverse problem of cyclographic modeling of a curve.
2. Optimal division of the given cyclographic projection $\overline{p}_c(t)$ into elements in order to construct the *MAT* curve is achieved when the boundary points of the elements are located at the vertex points of curve $\overline{p}_c(t)$.
3. Given a convex contour $\partial(\Omega)$, two of its points with highest curvature define the *MAT* curve boundaries.
4. Not every point of convex contour $\partial(\Omega)$ of curvature maximum defines the *MAT* curve boundaries, i.e. there may be lines of intersection of α-surfaces not included into the sought *MAT* curve.

3. Conclusion

The results of the study prove that given a plane domain boundary contour as a cyclographic projection of a spatial curve allows one to unambiguously construct the said curve. Compared to the known solutions, the proposed geometric model of solution to this problem has the advantages of simplicity and precision of calculation algorithm that provides an analytic solution to the problem given a boundary contour in the form of second-degree curves. For the case of more complex boundary contours, another algorithm providing analytical definition of the sought curve in the form of a discrete series of points is proposed.

4. References

[1] H. Pottmann, J. Wallner, Computational Line Geometry, Berlin, Springer Verlag, 2001.

[2] K. L. Panchuk, N. V. Kaygorodtseva, Cyclographic Descriptive Geometry, Omsk, OmGTU, 2017 (in Russian).

[3] K. L. Panchuk, E. V. Lyubchinov, T. M. Myasoedova, Computer aided geometric modeling of solutions to the tasks of applied cyclography, *CEUR Workshop Proceedings* (GraphiCon 2019, Computer Graphics and Vision). Vol. 2485 (2020), pp. 185-188.

[4] E. V. Lyubchinov, K. L. Panchuk, Geometric modeling of solutions of the direct and inverse tasks of geometric optics on a plane, IOP Conf. Series: Journal of Physics: Conf. Series. Vol. 1210 (2019), P. 012087. doi: 10.1088/1742-6596/1210/1/012087.

[5] C. Zezhong, F. Qiang, An efficient, accurate approach to medial axis transforms of pockets with closed free-form boundaries, Eng. Comp. 30 (2014), pp. 111–123. doi: 10.1007/s00366-012-0295-5.

[6] M. Held, On the Computational Geometry of Pocket Machining. Lecture Notes in Computer Science, Berlin : Springer Verlag Publ., 1991.

[7] H. I. Choi, C. Y. Han, H. P. Moon, K. H. Roh, N. S. Wee, Medial axis transform and offset curves by Minkowski Pythagorean hodograph curves, Comp.-Aided Des., 31 (1999), pp. 9–72.

[8] M. Ramanathan, B. Gurumoorthy, Constructing Medial Axis Transform of Planar Domains, Comp.-Aided Des., 6(21) (2003), pp. 371-378. doi: 10.1016/S0010-4485(02)00085-4.

[9] W. L. F. Degen, Exploiting curvatures to compute the medial axis for domains with smooth boundary, Comput, Comp.-Aided Des, 21 (2004), pp. 641–660. doi: doi.org/10.1016/j.cagd.2004.03.005.

[10] J. Peethambaran, A. D. Parakkat, R. Muthuganapathy, A Voronoi based Labeling Approach to Curve Reconstruction and Medial Axis, Approximation Computer Science PG, 2015, pp. 77-82. doi: 10.2312/pg.20151285.

[11] G. Berg, W. Julian, R. Mines, F. Richman, The constructive Jordan curve theorem, Rocky Mountain Journal of Mathematics, 5 (2) (1975), pp. 225–236. doi: 10.1216/RMJ-1975-5-2-225.

[12] N. N. Golovanov, Geometric modeling, Moskow: Fizmatlit, 2002 (in Russian).